

# Water and Salt Permeability of Reinforcement Polymer-Gel Composite Membrane

A. Mounir EL Sayed,<sup>1</sup> A. Yamauchi,<sup>2</sup> N. A. Darwish,<sup>1</sup> A. A. Abd EL-Mageed,<sup>1</sup> S. F. Halim<sup>1</sup>

<sup>1</sup>National Institute for Standards, Polymer Testing Laboratory, Al Haram 12211, Egypt

<sup>2</sup>Physics Division, Graduate School of Science, Kyushu University, Fukuoka 812-8581, Japan

Received 3 December 2007; accepted 12 March 2008

DOI 10.1002/app.28366

Published online 20 May 2008 in Wiley InterScience (www.interscience.wiley.com).

**ABSTRACT:** The charged mosaic polymer membrane (CMM) without reinforcement and the composite charged mosaic polymer membrane (CCMM) with reinforcement were investigated in terms of salt and water transport (permeability). The composite charged mosaic polymer membrane (CCMM) with reinforcement showed a unique transport behavior such as preferential material transport  $L_p$  and  $\omega$ . Water permeability coefficient,  $L_p$  and salt permeability coefficient,  $\omega$  were estimated by taking account of active layer thickness of composite polymer gel. The  $L_p$

and  $\omega$  values of CCMM with reinforcement were larger than those of CMM without reinforcement. On the other hand, the reflection coefficient of CCMM,  $\sigma$ , showed negative value, which suggested preferential material transport to solvent transport. © 2008 Wiley Periodicals, Inc. *J Appl Polym Sci* 109: 2988–2993, 2008

**Key words:** composite polymer membrane; permeability; negative reflection coefficient; transport number; active layer; reinforcement

## INTRODUCTION

Separation membranes have become essential part of human life because of their growing industrial applications such as biotechnology, nanotechnology, and membrane-based energy devices, in addition to different membrane-based various separation and purification process. The development of the charged membrane system with new functional groups is required to increase the efficiency in the desalination of seawater or to recover waste solutions containing heavy metals.<sup>1,2</sup> Mosaic-charged membranes have been proposed because this membrane is expected to be applied in many fields, e.g., food, medicine, and sea water that requires desalination.<sup>3–10</sup> The transport behavior of solvent and solute across the charged polymer membranes were reported<sup>11,12</sup> and the characteristics of the charged polymer membrane such as the preferential solute transport was observed as well.<sup>13</sup> Also, the comparison of transport properties of monovalent anions through anion exchange membranes and charge-mosaic polymer membrane prepared from microspheres were studied as well.<sup>13,14</sup> In this study, the transport material properties (permeability's) of composite charged mosaic polymer membrane, which contains cationic and anionic polymer gel microspheres with and without rein-

forcement were investigated. Furthermore from electrochemical aspect, the ionic mobility via membrane potential measurements of composite charged mosaic polymer membrane/electrolyte solution system was studied. The study of membrane potential provides the information regarding the transport behaviors of cation and anion in the membrane. Also to understand the material transport mechanism in mosaic polymer gel membrane from basic viewpoint, the results of charged composite mosaic polymer membrane (CCMM) with reinforcement are compared with the results of the charged mosaic polymer membrane without reinforcement.

## EXPERIMENTAL

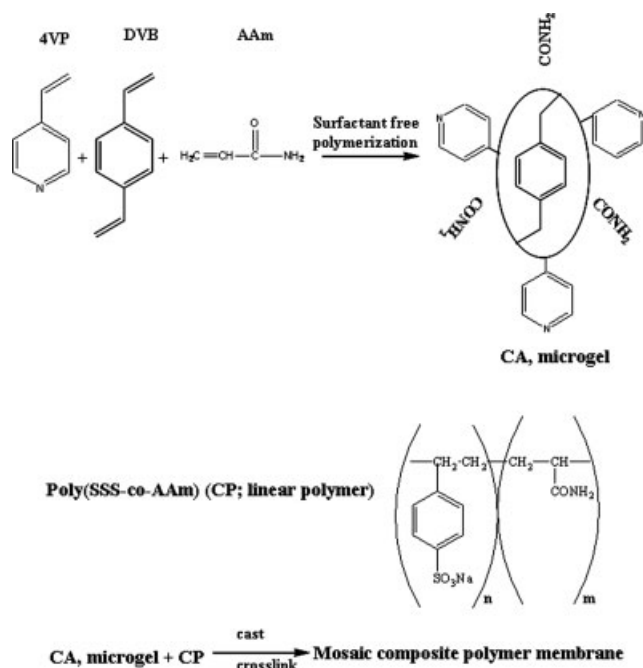
### Material

The 4-Vinylpyridine (4VP), sodium styrene sulfonate (SSS), divinylbenzene (DVB; *m* and *p* mixture, purity—55%), acrylamide (AAm), diiodobutane (DIB), iodomethane (MeI), glutaraldehyde (GA), and acetone were purchased from Tokyo Kasei. The 2,2'-Azobis(2-methylpropioamide)dihydrochloride (V50) was purchased from Wako Pure Chemicals, Japan. The 4VP was purified by distillation under reduced pressure before use.

### Preparation of the polymer microgel exchange components

Scheme 1 shows the synthetic procedure for the ion-exchange polymer microgel elements (CA and CP)

Correspondence to: A. M. EL Sayed (mounir\_99@yahoo.com).



**Scheme 1** Preparation of ion exchange polymer and mosaic membrane.

and the preparative procedure of the mosaic polymer membrane.<sup>15,16</sup>

### Anion-exchange polymer microgel component (CA)

The monomers, 4VP (10 mL), AAm (1 g), DVB (1 g), and initiator (GA) were added to 500 mL water. Under vigorous stirring, N<sub>2</sub> gas was bubbled at room temperature for 10 min. The polymerization was carried out at 70°C for 10 h. The obtained polymer solutions were purified by dialysis. CA was inner cross-linked microgels. CA had AAm as a unit, which was able to connect CA to the matrix. CA was quaternized after the formation (cast) of membranes.

### Cation-exchange polymer component (CP)

Poly(SSS-co-AAm) (CP; linear polymer) was prepared by the solution polymerization of styrene sodium sulfonate, SSS, (12 g) with acrylamide, AAm, (4 g) under an atmosphere of N<sub>2</sub> gas at 70°C for 12 h in 100 mL of deionized water; V50 (0.5 g) was used as an initiator. The obtained polymer solution was poured into a large excess of acetone. The precipitated polymer was further purified by dissolution in water and precipitation in acetone three times. The number-average molecular weight of the polymer was 45,000, and the weight-average molecular weight divided by the number average molecular weight was 3.2 (gel permeation chromatography; Toso TSK gel, PW type, Japan). CP was prepared for use as the matrix phase of the membrane.

### Preparation of the charge-mosaic membrane

An CA, poly(4-vinyl pyridine) (P4VP; microgel) dispersion in an aqueous solution and a solution containing CP and GA were mixed, and the dispersion was cast onto a glass Petridish and dried in air for 7 days. The CP matrix phase was crosslinked in an atmosphere of concentrated HCl vapor for 7 days. The membrane was soaked in an aqueous sodium acetate solution, washed with deionized water, and dried in air. The resulting membrane was simultaneously crosslinked by quaternization with DIB gas and methanol vapors for 7 days. The residual 4VP units were completely quaternized with Mel (4VP units quaternized by DIB and Mel were almost the same in moles, P4VP/PSSS composite membrane made (1.0/1.0) mol/mol). Schematic model of the charged composite mosaic polymer membrane with support (reinforcement) was shown in Figure 1. In this study, the mosaic membrane without support film, CMM, consists of only active layer. The "active layer" stands for a part of charged polymer gel structure in mosaic membrane. The total membrane thickness was measured by the thickness gauge to be about 50 μm. Lithium chloride (LiCl), sodium chloride (NaCl); potassium chloride (KCl) salts were purchased from ABIOS, Japan.

### Permeability studies

The used cell for experiment consisted of two half cells. The charged mosaic polymer membranes were tightly clamped between two half-glass cells by using silicon rubbers to avoid leak of solution from the contact position between membrane and the orifice of cells. Each cell volume was 25 mL and the effective membrane area was 3.14 cm<sup>2</sup>. Temperature of glass cells was kept at constant by circulating thermostated

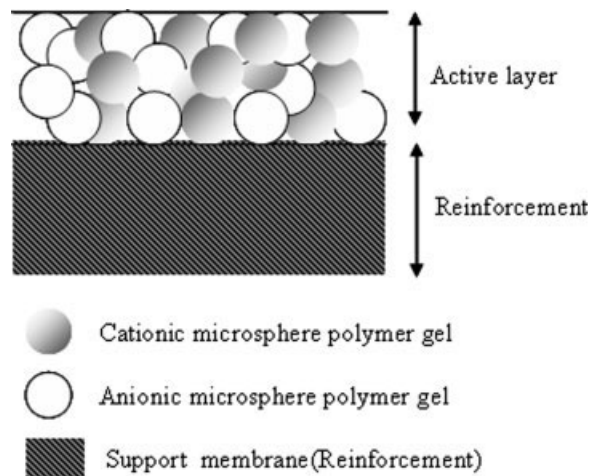


**Figure 1** Schematic model for composite charged mosaic polymer membrane, CCMM.

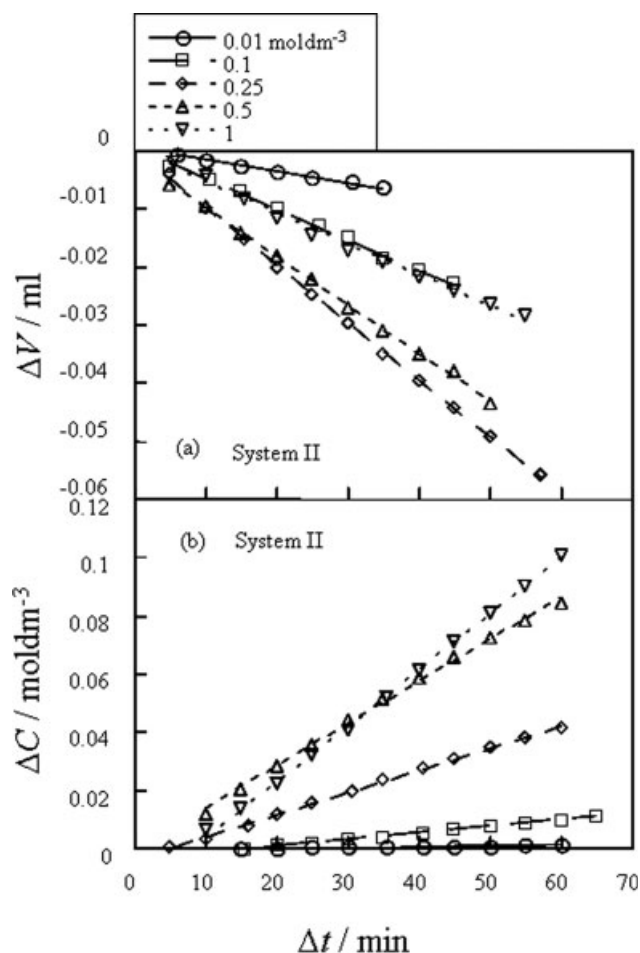


**Figure 2** (a) The volume change,  $\Delta V$  versus time,  $\Delta t$  in the case of CCMM with reinforcement in cell<sub>2</sub> of system II. (b) The concentration change,  $\Delta C$  versus time,  $\Delta t$ , in the case of CCMM with reinforcement in system II and Cell<sub>2</sub>.

water around the two cells during experiment. The volume change and salt concentration change were measured as function of time by using graduated glass capillary and pencil-type conductance electrode in cell<sub>1</sub> or cell<sub>2</sub>, respectively. Volume flux and solute flux were estimated from volume change versus time or concentration change versus time by taking account of membrane area, respectively.

#### System I

A 0.5 mol dm<sup>-3</sup> aqueous sucrose solution and distilled water were separately placed in both cell<sub>1</sub> and cell<sub>2</sub>, across the composite polymer gel charged mosaic membrane.

#### System II

This system, aqueous KCl solution and distilled water were inserted into cell<sub>1</sub> and cell<sub>2</sub>, respectively, and KCl concentrations were changed from 0.01 to 1 mol dm<sup>-3</sup>. The decrease of volume,  $\Delta V$  against time,

$\Delta t$  was determined as negative values. The dependence of  $\Delta V$  on the different salt concentration was observed (see Fig. 2). Also the dependence of the slope,  $\Delta V/\Delta t$ , which represented by  $J_v$ , on the different salt concentration was not linear as shown in Figure 3(a).

#### Cationic transport number, $t_+$ (ionic mobility)

Cationic transport number,  $t_+$  was deduced from membrane potential measurement. A pair of silver/silver chloride electrodes was inserted into both glass cells, and used for membrane potential measurements. The electrolyte concentrations in cell<sub>1</sub> were changed to 0.5, 0.025, 0.01, and 0.005 mol dm<sup>-3</sup> and that in cell<sub>2</sub> was kept constant at 0.05 mol dm<sup>-3</sup>. The potentials in each system were measured as a function of time by using a digital potentiometer (ORION RESEARCH, Microprocessor ionalyzer/901).

## RESULTS AND DISCUSSION

Figure 2(a,b) shows that the volume change, and KCl concentration change with time for CCMM,

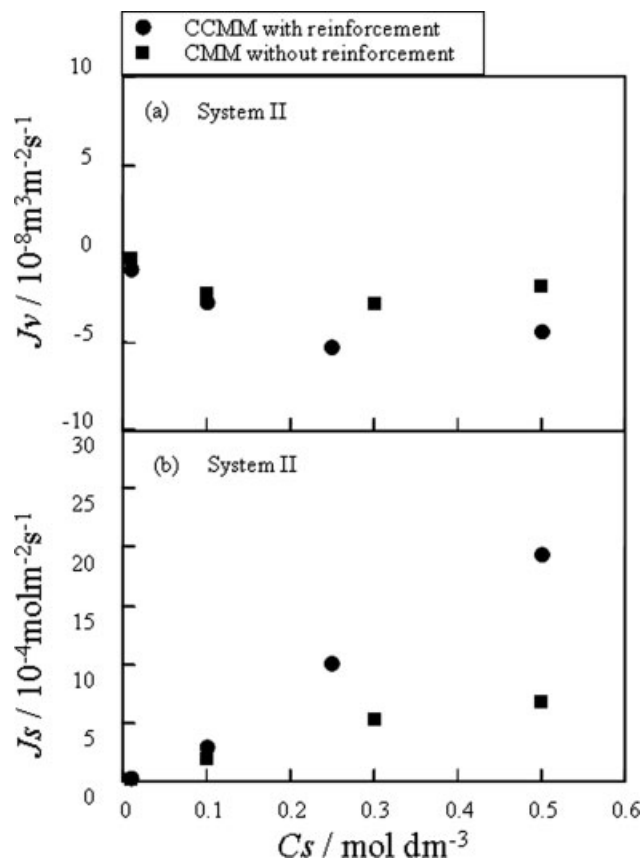


**Figure 3** Dependence of volume (a) and salt fluxes (b),  $J_v$  and  $J_s$  on added salt concentrations  $C_s$  of CMM with and without reinforcement in system II.

respectively. Figure 2(a) showed linear relationship with steady state in the range of the used time; however the direction of volume change of KCl proceeded in negative direction. This means that the water and KCl permeates through the mosaic polymer gel membrane due to the osmotic pressure that resulted from KCl concentration differences, and presence of cationic and anionic polymer functional groups as well.

#### Filtration coefficient $L_p$ , reflection coefficient $\sigma$ , and salt permeability coefficient $\omega$

The volume flux,  $J_v$  and solute flux  $J_s$ , were deduced from the slope of the linear relations of  $\Delta V$  and  $\Delta C$  versus time, respectively, by taking into account the effective membrane area. The solvent fluxes  $J_v$  and solute flux  $J_s$  of charged mosaic polymer membrane with and without reinforcement were plotted as function of KCl concentration in system II, and shown in Figure 3(a,b). The values of  $J_v$  and  $J_s$  were obtained from volume changes in time and salt concentration in time (Fig. 2), respectively. One can observe that the values of  $J_v$  showed negative sign due to the transport direction from pure water to solution, while  $J_s$  values showed positive sign due to the transport direction from solution to water. It can be mentioned that the  $J_v$  and  $J_s$  values of charged mosaic polymer membrane with and without reinforcement showed difference, especially near  $0.3 \text{ mol dm}^{-3}$  of KCl. Inserting the volume flux,  $J_v$  into eq. (1), the filtration coefficient,  $L_p$  was obtained.  $L_p$  represents water transport index (water permeability) across the mosaic polymer membrane in system I. The changes of the  $L_p$  values of CCMM with reinforcement together with the values of CMM without reinforcement in the presence of different KCl concentrations were shown in Figure 4(a). Figure 4(a) indicated that the CCMM membrane more permeable to the water than that of CMM one. Also Figure 4(a) showed that the water permeability values were almost independent on KCl concentrations in the range  $0\text{--}0.5 \text{ mol dm}^{-3}$ . It was found that even though the thickness of the used membrane in our study was  $50 \mu\text{m}$ , the  $L_p$  values of composite polymer membrane with reinforcement (CCMM) became larger than that of mosaic membrane without reinforcement (CMM). Figure 4(b,c) shows that the reflection coefficient,  $\sigma$  and salt permeability,  $\omega$  from the solvent and solute fluxes in system II, respectively. Using  $J_v$  and  $J_s$  values, and using eqs. (2) and (3), the  $\sigma$  and  $\omega$  values were deduced, respectively. Figure 4(b) showed that the  $\sigma$  values of CCMM with reinforcement and CMM without reinforcement were almost same. The relative ratio of solute velocity to solvent velocity,  $\sigma$ , showed negative values in the examined concentration ranges. The negative  $\sigma$

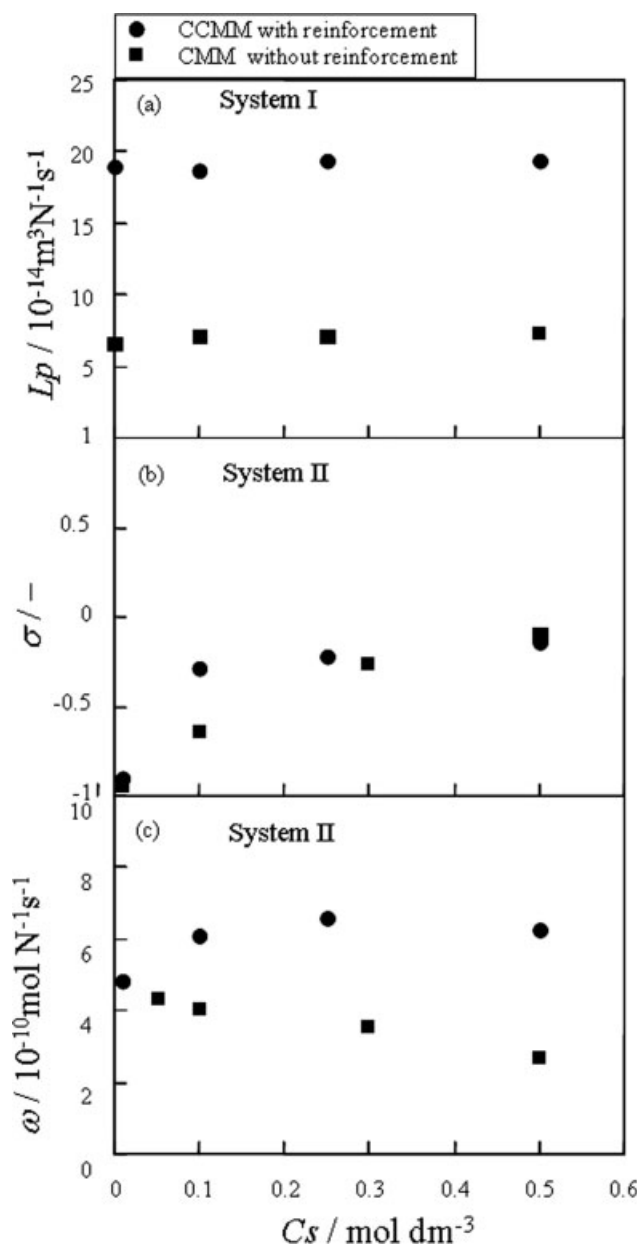


**Figure 4** (a) Dependence of water permeability's,  $L_p$ , (b) Reflection coefficients  $\sigma$ , and (c) salt permeability's,  $\omega$ , on salt concentrations for CMM with and without reinforcement.  $L_p$  values were estimated using eq. (1) assuming  $\sigma = 1$ . Reflection coefficient  $\sigma$  was obtained from volume fluxes using eq. (2). Salt permeability,  $\omega$  was obtained from salt fluxes using eq. (3).

values means that the preferential salt diffusion was enhanced over the water diffusion, which is very important for practical pressure dialysis process. The enhancement of the salt diffusion across the composite polymer membrane was attributed to the presence of cationic (PSSS) and anionic (P4VP) polymer exchange sites inside the mosaic membrane. On the other hand,  $\omega$ , salt permeability values were given as a function of KCl concentrations in Figure 4(c). Figure 4(c) showed a remarkable different between

the  $\omega$  values of charged mosaic polymer membranes with and without reinforcement. This means that the CCMM with reinforcement was more permeable to the KCl salt than CMM membrane without reinforcement as shown in Figure 4(c). Figure 4(a,c) suggest that the  $L_p$  and  $\omega$  values are possibly related to the active layer of composite polymer gel in the membrane. In the other words, the solvent (water) and solute (salt) transports depend strongly on the active layer thickness of polymer composite membrane. While the relative ratio of solute velocity to solvent velocity,  $\sigma$ , doesn't depend on the membrane thickness. This gives us the necessity to considering the active layer thickness of the polymer mosaic membrane that consists of composite polymer PSSS and P4VP active sites. From the fact mentioned above, the equations used for evaluation of  $L_p$ ,  $\sigma$ , and  $\omega$  didn't include a term of active layer thickness  $\delta$ . According to Kedem and coworkers,<sup>17,18</sup> membrane parameters,  $L_p$ ,  $\sigma$ , and  $\omega$  under appropriate experimental conditions were given as follows,

$$L_p = - \left( \frac{J_v}{\Delta\Pi} \right)_{\Delta P=0, \sigma=1}, \quad (1)$$

$$\sigma = - \frac{1}{L_p} \left( \frac{J_v}{\Delta\Pi} \right)_{\Delta P=0}, \quad (2)$$

$$\omega = \left( \frac{J_s}{\Delta\Pi} \right)_{J_v=0, \Delta P=0}. \quad (3)$$

The membrane parameters in Figure 4(a,c) were estimated using eqs. (1)–(3). As described above, the equations having a term of active layer thickness are needed to explain the discrepancy between CMM and CCMM. The equations, which predict the membrane thickness, are given in eqs. (6) and (7) as follows

$$J_v = \frac{L_{p'}}{\delta} (\Delta P - \sigma \Delta \Pi), \quad (4)$$

$$J_s = C_s^a (1 - \sigma) J_v + \frac{\omega'}{\delta} \Delta \Pi \quad (5)$$

Comparing eqs. (1)–(3) with eqs. (4) and (5), one can obtain the relation between present and previous  $L_p$  and  $\omega$  as follows,

$$L_{p'} = L_p \cdot \delta, \quad (6)$$

$$\omega' = \omega \cdot \delta. \quad (7)$$

Equations (6) and (7) indicate that the transport quantities  $L_p$  and  $\omega$ , across the mosaic polymer membrane are inversely proportional to the membrane thickness. By considering the membrane thick-

ness 50  $\mu\text{m}$  as reference, and using eq. (6), the thickness of the active layer of CCMM was estimated as 18.5  $\mu\text{m}$ . The higher values of  $L_p$  and  $\omega$  of CCMM with reinforcement compared to that of CMM without reinforcement are possibly explained based on the thickness of the active layer of membrane (18.5  $\mu\text{m}$ ). As the membrane thickness gets thinner (18.5  $\mu\text{m}$ ) the functional groups of cationic and anionic polymer ( $\text{SO}_3^-$  group of PSSS, and methyl iodide pyridine group of P4VP) are preferentially pointed up toward the surface.<sup>19</sup> This may increase the activity of the membrane due to the presence of anionic and cationic polymer functional groups near to the membrane surface, which led to an increase in the permeability properties  $L_p$  and  $\omega$  of CCMM with reinforcement. On the other hand, at larger membrane thickness (50  $\mu\text{m}$ ) the functional groups of cationic and anionic polymer functional groups are migrated into the bulk of membrane<sup>19</sup> due to the polymer chains entanglement.<sup>20</sup> So, the functional groups of cationic and anionic polymer are decreased near to the mosaic membrane surface, and accordingly led to a decrease in the membrane activity, i.e., decrease its transport properties.

### Reproduction of $J_v$ and $J_s$

To verify the effect of the active layer thickness of composite polymer membrane, CCMM on the transport properties,  $J_v$  and  $J_s$  of the composite polymer membrane were reproduced from the previous results by using the thickness of active layer as 18.5  $\mu\text{m}$ , and shown in Figure 5(a,b). As shown in Figure 5(a,b) the predicted solid lines were satisfactorily fitted with the experimental results of composite charged mosaic membrane, CCMM. Regarding to the minimum observed around 0.3 mol dm<sup>-3</sup> in Figure 5(a). At relative dilute salt concentration range, the diffusion force due to presence of both cationic and anionic polymer dominates over osmotic force. However at higher salt concentration range, the osmotic flow due to salt concentration difference dominates the total flow. As a result, the composite charged mosaic membrane (CCMM) was exhibited an excellent transport performance.

### Cationic transport number, $t_+$ (ionic mobility)

From membrane potential measurements, the transport numbers of cation,  $t_+$  were estimated by using Nernst equations. The  $t_+$  gives the index of ionic mobility of cation inside the polymer membrane with and without reinforcement. The  $t_+$  values of LiCl, NaCl, and KCl didn't show remarkable difference between CCMM with reinforcement and CMM without reinforcement (0.49, 0.45, 0.55). This indicates that both  $\text{K}^+$  and  $\text{Cl}^-$  ions permeate easily within

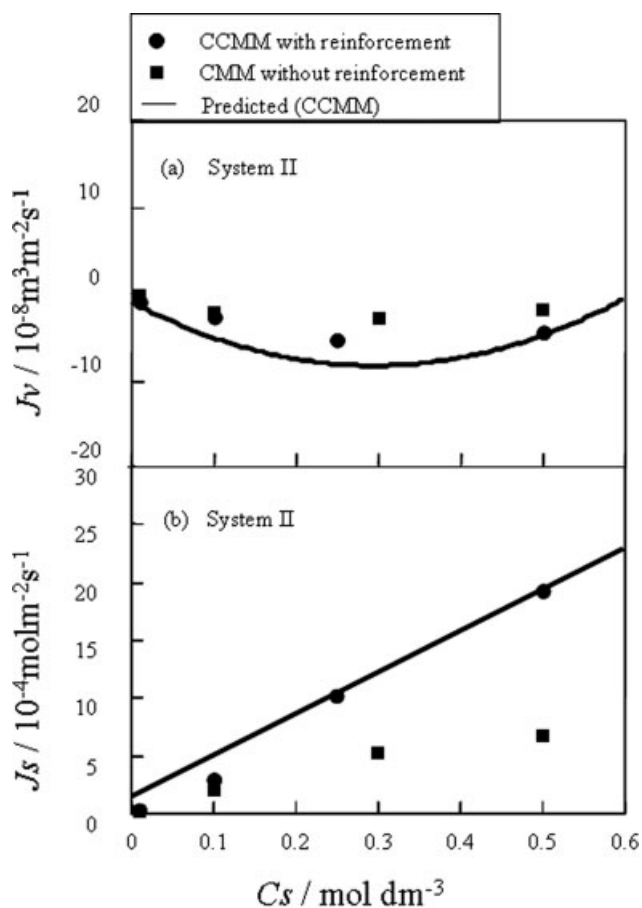


**Figure 5** Comparison of the experimental data of  $J_v$  (a) and  $J_s$  (b) values of CMM with and without reinforcement with predicted one. Solid lines indicate the predicted data from eqs. (6) and (7).

composite polymer membrane due to the presence of two active sites of cationic and anionic polymer inside the membrane. One can conclude that the mobility of ions in the membranes, CCMM and CMM behaves approximately in the same manner.

### CONCLUSIONS

The water transport,  $L_p$  and salt transport,  $\omega$  values in CCMM membranes with reinforcement showed larger values than those of CMM membrane without reinforcement. In the other words,  $L_p$  and  $\omega$  transports were depended strongly on the active layer

thickness of polymer composite membrane, while the relative ratio of solute velocity to solvent velocity,  $\sigma$ , didn't depend on the membrane thickness. The negative  $\sigma$  values were attributed to the enhancement of the salt diffusion across the membrane. This salt diffusion across the polymer gel mosaic membrane was explained in terms of the presence of cationic and anionic polymer exchange sites inside the mosaic membrane. Also, the mosaic composite polymer membrane was reinforced without losses of original properties of charged mosaic membrane. A composite charged mosaic polymer membrane might be potentially used for pressure dialysis and desalination.

### References

1. Fuqiang, L.; Guoqiang, L.; Chao-Yang W. *J Membr Sci* 2007, 287, 126.
2. Minoru, T.; Yoshifumi, S.; Michiei, N.; Shojiro, H.; Takashi, F. *J Polym Sci Part A: Polym Chem* 2003, 41, 1251.
3. Weinstein, J. N.; Caplan, S. R. *Science* 1968, 161, 70.
4. Weinstein, J. N.; Caplan, S. R. *Science* 1970, 169, 296.
5. De Korosy, F.; Shorr, J. *Nature* 1963, 197, 685.
6. Chapiro, A.; Jendrychowska, A. M.; Mizrahi, S. *Eur Polym Mater* 1976, 12, 773.
7. Chapiro, A.; Jendrychowska, A. M. *Polym Eng Sci* 1980, 20, 202.
8. Ishizu, K.; Inagaki, K.; Fukutomi, T. *J Polym Sci Polym Chem Ed* 1985, 23, 1099.
9. Kawatoh, H.; Hakimoto, M.; Tanioka, A.; Inoue, T. *Macromolecules* 1988, 21, 625.
10. Junsheng, L.; Tongwen, X.; Ming, G.; Yanxun, F. *J Membr Sci* 2005, 260, 26.
11. Fukuda, T.; Yamauchi, A. *Bull Soc Sea Water Sci Jpn* 2002, 56, 41.
12. Yamauchi, A.; Fukuda, T. *Ann N Y Acad Sci (Adv Membr Technol)* 2003, 984, 256.
13. Abdulah, E.; Azzedine, E.; Natalia, P.; Claude, G.; Gerald, P. *J Membr Sci* 1998, 143, 249.
14. Minory, T.; Yoshifumi, S.; Naomi, O.; Michiei, N.; Shojiro, H.; Takashi, F. *J Polym Sci Part A: Polym Chem* 2003, 41, 1251.
15. Fukutomi, T.; Nakamura, M.; Takizawa, M.; Sugito, Y.; Doi, S.; Oguma, N.; Takeuchi, H.; Maruyama, M.; Mizoguchi, T.; Horiguchi, S. *Jpn Kokai Tokkyo Koho JP10087855*.
16. Takizawa, M.; Sugito, Y.; Oguma, N.; Nakamura, M.; Horiguchi, S.; Fukutomi, T. *J Polym Sci Part A: Polym Chem* 2003, 41, 1251.
17. Kedem, O.; Katchalsky, A. *Trans Faraday Soc* 1963, 59, 1931.
18. Katchalsky, A.; Curran, P. F. *Nonequilibrium Thermodynamics in Biophysics*, Harvard University Press: New York; 1965.
19. EL Sayed, A. M.; Kajiyama, T. *Polym J* 1999, 31, 89.
20. EL Sayed, A. M.; Kajiyama, T. *Polym J* 1999, 31, 550.